

# Recent Advances in the Dynamics of Single Crystal to Single Crystal Transformations in Metal–Organic Open Frameworks

Myunghyun Paik Suh<sup>A,B</sup> and Young Eun Cheon<sup>A</sup>

<sup>A</sup> Department of Chemistry, Seoul National University, Seoul 151-747, Korea.

<sup>B</sup> Corresponding author. Email: mpsuh@snu.ac.kr

Single crystal to single crystal transformations have been the subject of growing interest in recent years. In this article, several examples of single crystal to single crystal transformations that occur in metal–organic open frameworks (MOFs) upon guest removal and rebinding, guest exchange, and chemical oxidation are introduced. Depending on the structures of the MOFs, host framework structures can be retained or altered upon guest removal. When host framework structures are altered, significant rearrangements of the molecular components, which involve sponge-like shrinkage/swelling, sliding, swing, bending, and/or rotational motions, occurs throughout the entire crystal to retain the single crystallinity.

Manuscript received: 16 January 2006.

Final version: 3 June 2006.

## Introduction

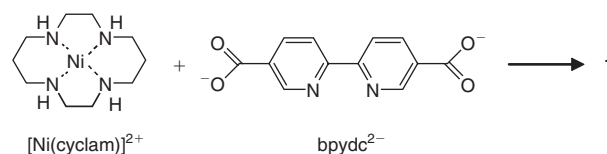
Metal–organic open frameworks (MOFs) with well-defined channels or pores have attracted great attention because they have the potential to be applied in adsorption and separation processes,<sup>[1–10]</sup> gas storage,<sup>[6,11–13]</sup> ion exchange,<sup>[14,15]</sup> heterogeneous catalysis,<sup>[16,17]</sup> and sensor technology.<sup>[18,19]</sup> Recently, it has been shown that they can be employed to fabricate small-sized silver and gold nanoparticles that are difficult to obtain by conventional methods.<sup>[20,21]</sup>

MOFs with various structures can be assembled from a wide variety of metal ions and organic building blocks. In MOFs, the pores and channels are filled with guest molecules, and the frameworks are often collapsed when the guest molecules are removed. In addition, single crystals of MOFs are frequently broken into small pieces and lose transparency when they are heated or evacuated. However, it has recently been found that some MOFs show single crystal to single crystal (SC–SC) transformations on removal, reintroduction, and exchange of the guest molecules as well as on chemical redox reactions. Some transform without a change of the framework structures,<sup>[6,22–29]</sup> but some do with a change in the framework structures by the extensive movements of the molecular components involving sponge-like shrinkage/swelling, sliding, swing, bending, and/or rotational motion.<sup>[12,30–38]</sup> Compounds that transform in the single crystal to single crystal manner, particularly the ones that transform reversibly, are important for the development of new and technologically useful materials including devices and sensors.

## SC–SC Transformation of a 3D Porous Framework Constructed of 1D Coordination Polymer Chains: Retention of Framework Structure on Desolvation and Resolvation Accompanied with Colour Change

A one-dimensional coordination polymer,  $\{[\text{Ni}(\text{cyclam})(\text{bpydc})]\cdot 5\text{H}_2\text{O}\}_n$  **1**, has been assembled from the  $\text{Ni}^{\text{II}}$  macrocyclic complex  $[\text{Ni}(\text{cyclam})](\text{ClO}_4)_2$  and  $\text{bpydc}^{2-}$  ( $\text{bpydc}^{2-} = 2,2'$ -bipyridyl-5,5'-dicarboxylate) in water (Scheme 1).<sup>[6]</sup>

In one-dimensional coordination polymers, the  $\text{bpydc}^{2-}$  ligand is planar and locates almost perpendicularly to the coordination plane of the macrocycle (dihedral angle  $85.1(1)^\circ$ ), which creates grooves between the macrocycles as shown in Fig. 1. In the crystal structure, there are three series of one-dimensional coordination polymer chains that extend in three different directions, and they pack as a double network of three-fold braids<sup>[39]</sup> (Fig. 1): Two three-fold braids of slanting rods are packed with inversion of the braids on translation in the perpendicular direction. When they pack, all the macrocycles and the grooves fit in a key-and-lock style to furnish an extraordinarily robust framework.



Scheme 1. Self-assembly of **1**.

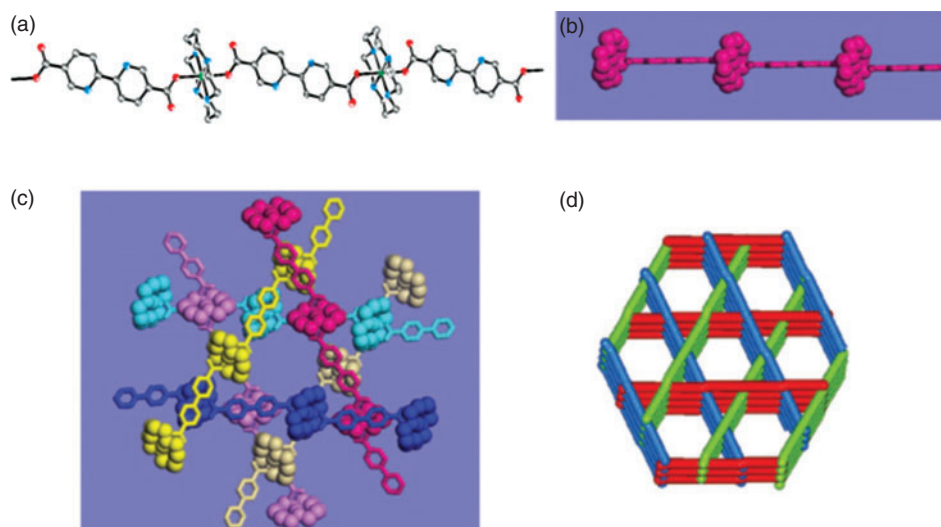
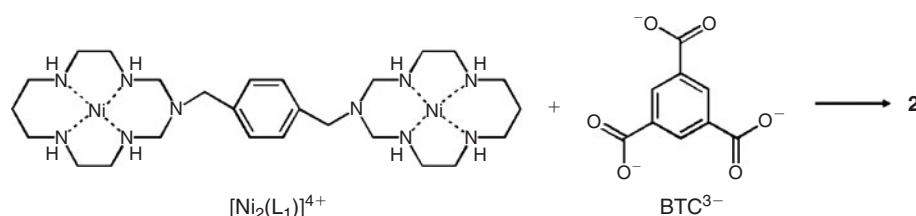
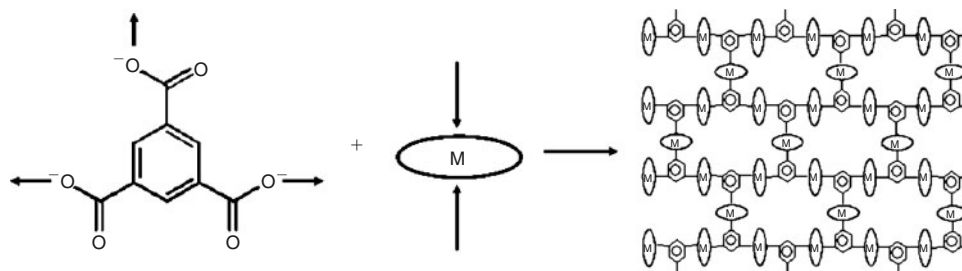


**Fig. 1.** The X-ray structure of **1**. (a) An *ORTEP* view for the linear coordination polymer chain. (b) A CPK view of (a), showing the formation of grooves between the macrocyclic units. (c) Double network of three-fold braids where macrocycles fit into the grooves created by  $\text{bpydc}^{2-}$ . (d) A view showing the stacking of the linear chains that generates one-dimensional channels.



**Scheme 2.** Self-assembly of **2**.



**Scheme 3.** Self-assembly of a two-dimensional network with brick-wall cavities.

The one-dimensional chains interact with one another by the  $\text{CH} \cdots \pi$  interactions between the carbon atom of the macrocycle and the pyridyl ring of  $\text{bpydc}^{2-}$ . The stacking of one-dimensional coordination polymer chains generates one-dimensional channels with honeycomb-like openings of 10.0 Å diameter (effective size 5.8 Å). The channels are filled with guest water molecules. The solid is stable up to 300°C. Solid **1** exhibits permanent porosity by adsorbing  $\text{N}_2$  gas, to show a reversible type I isotherm. The Langmuir surface area and pore volume are 817  $\text{m}^2 \text{g}^{-1}$  and 0.37  $\text{cm}^3 \text{cm}^{-3}$ , respectively.

Solid **1** is so robust that single crystallinity as well as the packing structure is retained during the many cycles of dehydration and rehydration processes. When crystal **1** is heated

at 150°C under  $10^{-5}$  torr for 2–40 h, it is dehydrated to give rise to a crystal of  $[\text{Ni}(\text{cyclam})(\text{bpydc})]_n$  (**1'**). In this dehydration process, the colour changes from yellow to pink. On exposure to moisture it returns to yellow very quickly (within 5 min for the crystal, immediately for the powder) to provide rehydrated crystal (**1''**). The X-ray crystal structures of **1'** and **1''** indicate that packing structures remain intact but bond lengths and angles that involve the  $\text{Ni}^{\text{II}}$  centre and the carboxylate ligand are slightly changed. When water guests are included in the channels, the axial Ni–O bond distances are slightly lengthened (0.025 Å), but it is not enough to explain the yellow colour that corresponds to the square-planar  $\text{Ni}^{\text{II}}$  species. In the X-ray crystal structures of **1**, **1'**, and **1''**, all  $\text{Ni}^{\text{II}}$  ions are in a pseudo-octahedral coordination geometry,

**Table 1.** Crystallographic parameters of **2**<sup>A</sup>

Parameter	<b>2</b>	<b>2'</b>	<b>2''</b>	<b>2-1</b>	<b>2-2</b>	<b>2-3</b>
Space group	$P\bar{1}$	$P\bar{1}$	$P1$	$P\bar{1}$	$P\bar{1}$	$P\bar{1}$
<i>a</i> [Å]	16.505	16.420	12.382	16.467	16.460	16.434
<i>b</i> [Å]	19.945	19.817	16.375	20.134	19.849	19.914
<i>c</i> [Å]	20.664	20.439	19.952	20.720	20.419	20.338
$\alpha$ [°]	73.00	70.32	74.51	72.53	70.50	71.26
$\beta$ [°]	68.24	68.55	89.26	67.94	71.08	70.07
$\gamma$ [°]	76.07	76.19	84.18	75.04	76.30	74.83
<i>V</i> [Å <sup>3</sup> ]	5974.3	5777.9	3877.9	5990.4	5887.0	5837.8
Bilayer thickness [Å]	11.91	11.27	6.82	11.71	11.75	11.75

<sup>A</sup> *R*<sub>1</sub> (unweighted, based on *F*<sup>2</sup>) values are 0.0899 for **2**, 0.1839 for **2'**, 0.1491 for **2''**, 0.1279 for **2-1**, 0.1299 for **2-2**, and 0.1547 for **2-3**.<sup>[30,31]</sup>

and they should show a pink colour. It seems that guest molecules affect the spectroscopic properties of the host, although we do not have the appropriate theory to explain the phenomena.

### SC-SC Transformation of a Pillared Bilayer Network Showing Sponge-Like Dynamics on Guest Removal and Rebinding

A pillared bilayer network,  $\{[\text{Ni}_2(\text{L}_1)]_3[\text{BTC}]_4 \cdot 6\text{pyr} \cdot 36\text{H}_2\text{O}\}_n$  (**2**;  $\text{L}_1 = \text{C}_{26}\text{H}_{52}\text{N}_{10}$ , pyr = pyridine), has been assembled from a  $\text{Ni}^{\text{II}}$  bismacrocylic complex  $[\text{Ni}_2(\text{L}_1)]^{4+}$  and  $\text{BTC}^{3-}$  ( $\text{BTC}^{3-} = 1,3,5\text{-benzenetricarboxylate}$ , Scheme 2).<sup>[30,31]</sup>

The X-ray crystal structure of **2** indicates that each  $\text{Ni}^{\text{II}}$  macrocylic unit is coordinated with two  $\text{BTC}^{3-}$  ions at *trans*-positions, and each  $\text{BTC}^{3-}$  ion binds three  $\text{Ni}^{\text{II}}$  ions that belong to three different bismacrocylic units through *C*<sub>1</sub> symmetry (Scheme 3). This results in two two-dimensional layers with a brick-wall motif of size  $22.6 \text{ Å} \times 14.3 \text{ Å}$ . The *p*-xylyl groups of the bismacrocycle act as pillars to link these two layers together to construct a pillared bilayer network (Fig. 2). The thickness of the bilayer is  $11.91(1) \text{ Å}$ . The bilayers are closely packed by fitting the grooves together. Solid **2** contains three-dimensional channels since the channels are created from top to bottom as well as the side directions. The aromatic rings of the *p*-xylyl pillars are positioned regularly almost parallel and perpendicularly to the direction of the side channels. The channel window size on the side of the bilayer is  $14.52(1) \text{ Å}$  (the effective channel width corrected for van der Waals surface is  $11.12(1) \text{ Å}$ ). The voids of the channels occupy 61% of the total volume as estimated by *PLATON*, and are filled with guest molecules.

When the single crystal of **2** is allowed to stand in air for 2 h and then heated at  $75^\circ\text{C}$  for 1.5 h,  $\{[\text{Ni}_2(\text{L}_1)]_3[\text{BTC}]_4 \cdot 30\text{H}_2\text{O}\}_n$  **2'** and  $\{[\text{Ni}_2(\text{L}_1)]_3[\text{BTC}]_4 \cdot 4\text{H}_2\text{O}\}_n$  **2''** result with retention of the single crystallinity. Crystallographic parameters, which include the cell volume, change significantly during this transformation as shown in Table 1. The X-ray crystal structures of **2'** and **2''** reveal that two-dimensional layers are intact, but the interlayer distance is reduced to 11.2 and  $6.8 \text{ Å}$ , respectively. In **2''**, the

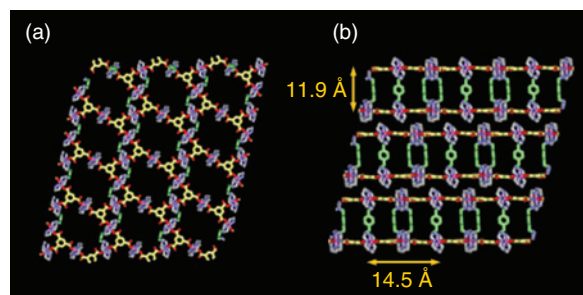


**Fig. 2.** The X-ray crystal structure of **2**. (a) Top view showing two-dimensional layers of a brick-wall motif of size  $22.6 \text{ Å} \times 14.3 \text{ Å}$ . (b) Side view showing the pillared-bilayer structure (bilayer thickness  $11.91(1) \text{ Å}$ ). Colour scheme: Ni pink, O red, N blue, C of macrocycle gray, C of  $\text{BTC}^{3-}$  yellow, C of pillars green. Guest water and pyridine molecules are omitted for clarity.

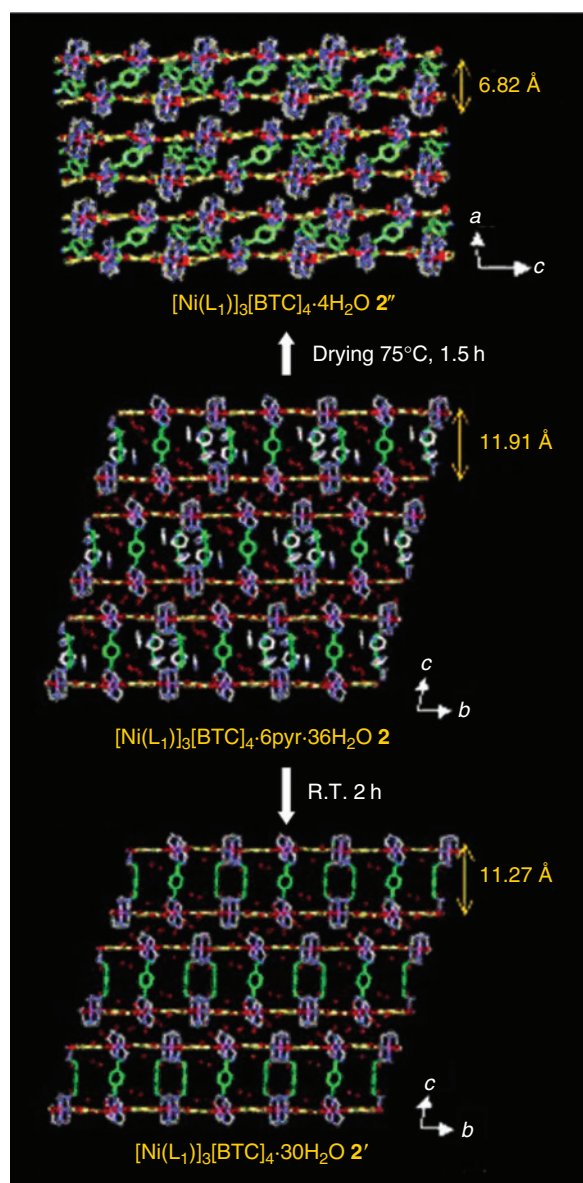


**Fig. 3.** The X-ray crystal structures of **2**, **2'**, and **2''**, which exhibit sponge-like behaviour of the single crystal in response to the amount of guest molecules included in the channels.



xylyl pillars are significantly tilted on removal of most of the guest molecules (Fig. 3). The results exhibit a novel sponge-like dynamic behaviour of the crystal that shrinks and swells depending on the amount of guest molecules included in the channels.

### SC-SC Transformation of a Pillared Bilayer Network on Guest Exchange

Pillared bilayer network **2** also undergoes a guest-exchange process in the SC-SC manner with pyridine and benzene in which solid **2** is completely insoluble. When crystal **2** is immersed in pyridine and benzene, parts of the guest molecules in **2** are exchanged to give rise to  $\{[\text{Ni}_2(\text{L}_1)]_3[\text{BTC}]_4 \cdot 20\text{pyr} \cdot 6\text{H}_2\text{O}\}_n$  (**2-1**) and  $\{[\text{Ni}_2(\text{L}_1)]_3[\text{BTC}]_4 \cdot 14\text{C}_6\text{H}_6 \cdot 19\text{H}_2\text{O}\}_n$  (**2-2**), respectively.

In **2-1**, pyridine molecules are included in the channels of the framework by face-to-edge  $\pi$ - $\pi$  interactions with the phenyl rings of  $\text{BTC}^{3-}$  of the two-dimensional layers and with the aromatic ring planes of the pillars. They are also intercalated between the bilayer units by hydrogen-bonding interactions with the host. In **2-2**, benzene molecules are included only in the channels by the  $\pi$ - $\pi$  interactions with the host. The size of the brick-wall motif of the two-dimensional layer and the thickness of the bilayer in guest-exchanged structures are unaltered compared with those in **2**. Retention of the single crystallinity upon this guest-exchange process must be attributed to the existence of three-dimensional channels in the framework, which offer no stress to the crystal during the guest-exchange processes.

### SC-SC Transformation of a Pillared Bilayer Network on Redox Reaction with Iodine

The coordination polymer solid that incorporates the  $\text{Ni}^{\text{II}}$  macrocyclic complex can be oxidized, because the  $\text{Ni}^{\text{II}}$  species can react with an oxidizing agent to become a  $\text{Ni}^{\text{III}}$  species that can be stabilized by the macrocyclic ligand and extra anionic axial ligands, even though  $\text{Ni}^{\text{III}}$  is in an unusually high oxidation state.<sup>[40]</sup>

When the crystal of **2** is immersed in a dimethyl sulfoxide (DMSO)/ $\text{H}_2\text{O}$  solution of  $\text{I}_2$ , it reacts with  $\text{I}_2$  while retaining the single crystallinity to produce  $\{[\text{Ni}_2(\text{L}_1)]_3[\text{BTC}]_4(\text{I}_3)_4 \cdot 5\text{I}_2 \cdot 17\text{H}_2\text{O}\}_n$  (**2-3**). The cell parameters of

**2-3** are not significantly altered compared with those of **2** (Table 1), even though its density ( $1.359 \text{ g cm}^{-3}$ ) is increased remarkably ( $\sim 28\%$ ) relative to that of **2** ( $1.061 \text{ g cm}^{-3}$ ).<sup>[31]</sup>

The X-ray crystal structure of **2-3** (Fig. 4) indicates that two-thirds of the  $\text{Ni}^{\text{II}}$  ions are oxidized to  $\text{Ni}^{\text{III}}$  to form a positively charged framework, and  $\text{I}_2$  molecules are reduced to  $\text{I}_3^-$  anions that are included in the channels. The two nickel ions that belong to the same bismacrocyclic complex are in the same oxidation state. The Ni-N and Ni-O bond distances involving  $\text{Ni}^{\text{III}}$  are shorter than those involving  $\text{Ni}^{\text{II}}$  ions. The presence of  $\text{Ni}^{\text{III}}$  ions in the framework is also evidenced by the electron paramagnetic resonance (EPR) spectra, which show anisotropic signals at  $g_{\parallel} = 2.024$  and  $g_{\perp} = 2.182$ , as well as the variable temperature magnetic susceptibility data of  $\mu_{\text{eff}} = 5.26 \mu_{\text{B}}$  at 301 K, which corresponds to the spin diluted system having four low spin  $\text{Ni}^{\text{III}}$  and two  $\text{Ni}^{\text{II}}$  ions per formula unit. Even though many  $\text{I}_3^-$  ions and  $\text{I}_2$  molecules are introduced into the channels of **2-3**, the thickness of the bilayer ( $12.20(1) \text{ \AA}$ ) is little changed compared with that of **2** ( $11.91(1) \text{ \AA}$ ). The two-dimensional layers are unaltered. Although this redox reaction involves oxidation of the framework, the introduction of  $\text{I}_3^-$  anions in the channels, and a 30% increase in the crystal density, the single crystallinity can be retained because of the existence of the three-dimensional channels in the framework.

### SC-SC Transformation Involving Rotational Motion of Molecular Components on Desolvation and Resolvation

It is a challenge to assemble porous MOFs that mimic the topology of conventional inorganic solids.<sup>[41,42]</sup> The MOFs with  $\text{PdF}_2$  or rutile net topology (Scheme 4) are interesting because they may be constructed by the combination of triangular and octahedral building blocks. Moreover, the assembly of such (3,6)-connected nets has been known to be difficult.<sup>[42]</sup>

A three-dimensional porous MOF,  $\{[\text{Zn}_4\text{O}(\text{NTB})_2] \cdot 3\text{DEF} \cdot \text{EtOH}\}_n$  **3**, has been prepared by the solvothermal reaction of  $\text{Zn}(\text{NO}_3)_2 \cdot 6\text{H}_2\text{O}$  and 4,4',4''-nitrilotrisbenzoic acid ( $\text{H}_3\text{NTB}$ ), which is carried out at  $110^\circ\text{C}$  in a mixture of DEF/EtOH/ $\text{H}_2\text{O}$  (5/3/2, v/v/v) for 24 h.<sup>[12]</sup> In the X-ray structure of **3**, the  $\text{Zn}_4\text{O}(\text{CO}_2)_6$  cluster and

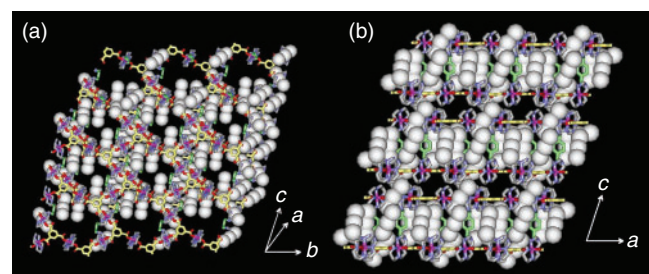
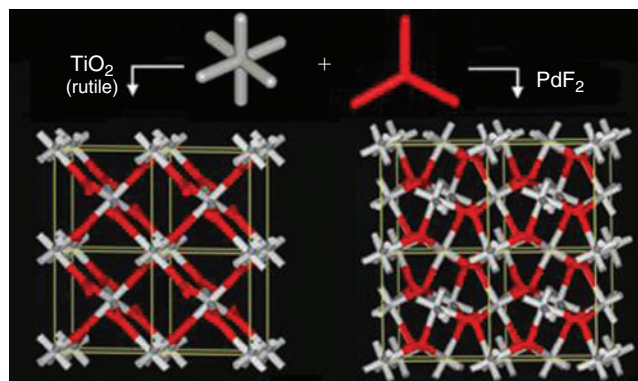


**Fig. 4.** The X-ray crystal structure of **2-3**, which shows the oxidized framework with  $\text{I}_3^-$  and  $\text{I}_2$  included in the channels. (a) Top view. (b) Side view. Colour scheme: Ni pink, O red, N blue, C of macrocycle gray, C of  $\text{BTC}^{3-}$  yellow, C of xylyl pillars green, I white. Guest water molecules are omitted for clarity.



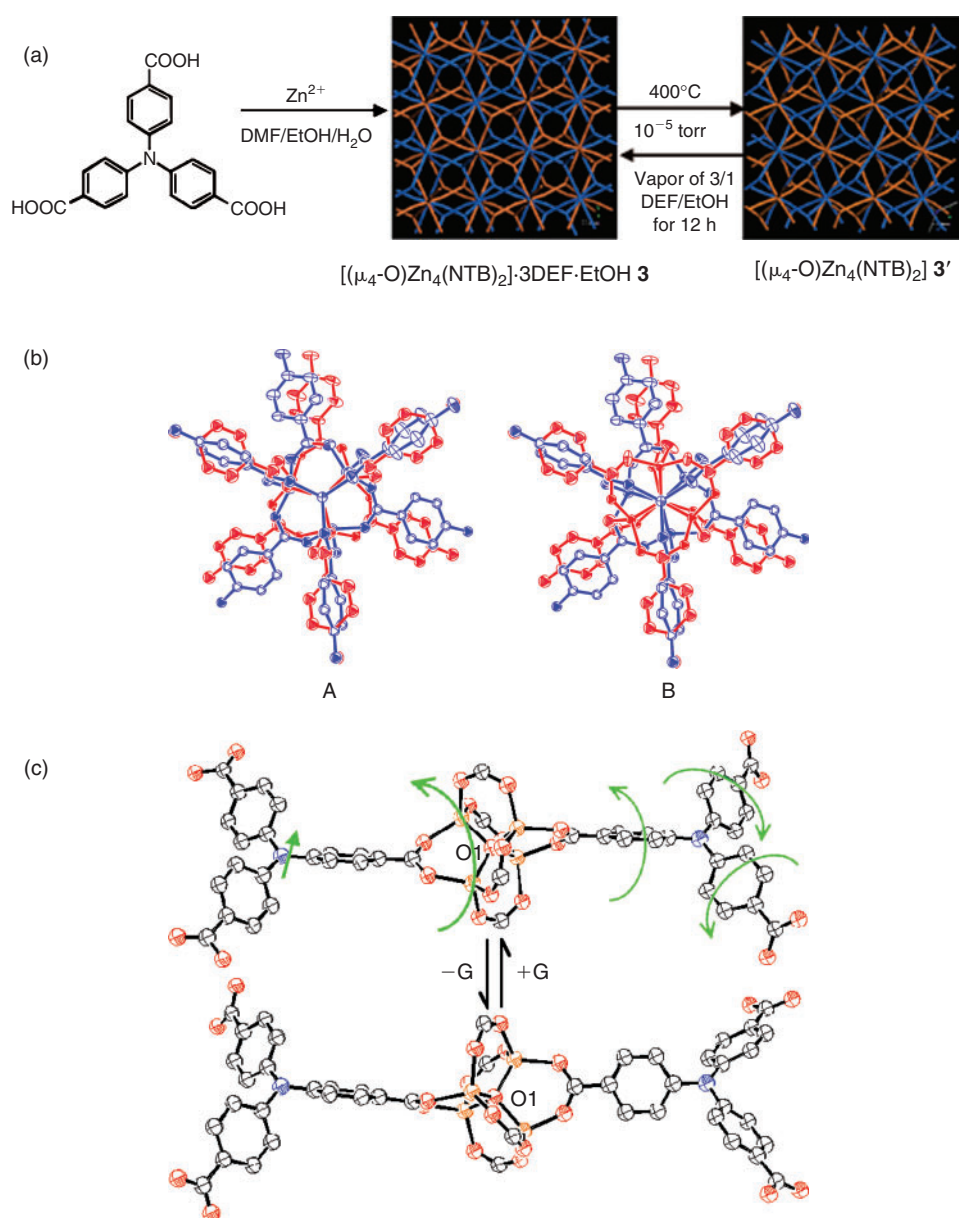
**Scheme 4.** Structures of  $\text{TiO}_2$  and  $\text{PdF}_2$  nets.

NTB<sup>3−</sup> act as an octahedral secondary building unit (SBU) and a triangular organic building block, respectively, which extend infinitely to give rise to a (3,6)-connected PdF<sub>2</sub> net. The nets are doubly interpenetrated to generate the curved three-dimensional channels. The void volume calculated by *PLATON* is 39.7%.

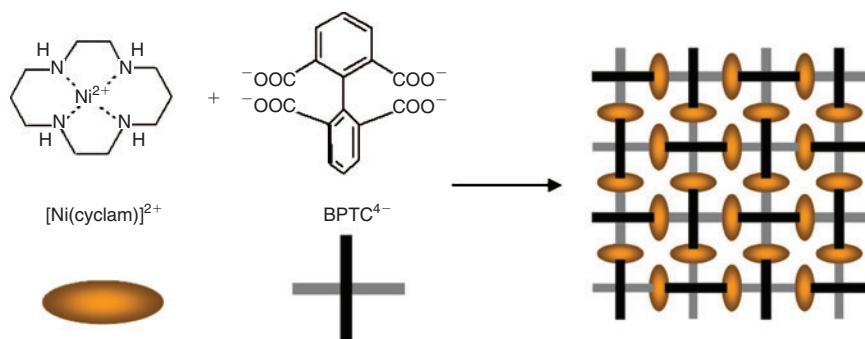
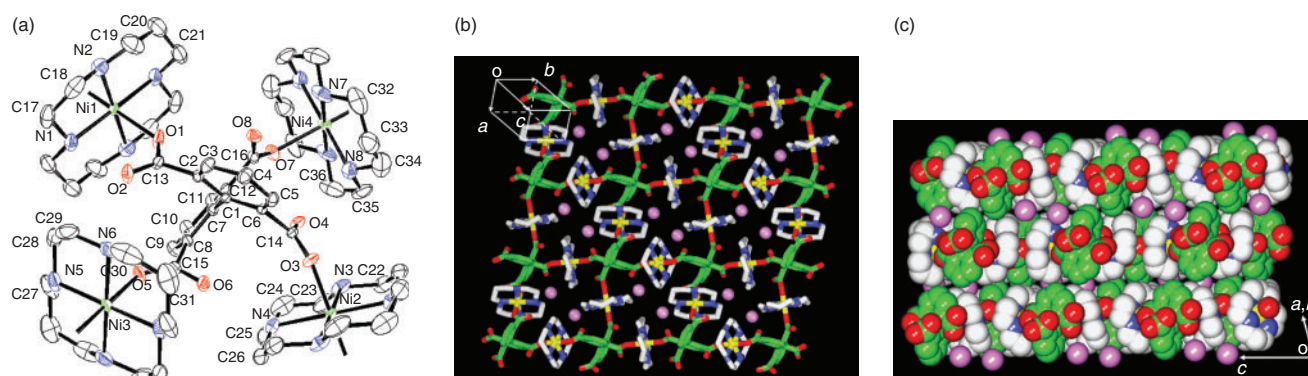
Framework **3** exhibits high permanent porosity (Langmuir surface area 1121 m<sup>2</sup> g<sup>−1</sup>, pore volume 0.51 cm<sup>3</sup> cm<sup>−3</sup>), high thermal stability (up to 430°C), high H<sub>2</sub> gas adsorption capacity (1.9 wt.-% at 77 K and 1 atm), selective organic guest binding ability (*K<sub>f</sub>*: MeOH > pyridine > benzene > dodecane),

and guest-dependent luminescence ( $\lambda_{\text{max}}$  depending on the guest identity).

Crystal **3** retains its single crystallinity as well as transparency even when it is desolvated at 400°C and 10<sup>−5</sup> torr for 0.5 h, which provides the single crystal of apohost [Zn<sub>4</sub>O(NTB)<sub>2</sub>]<sub>n</sub> **3'**. The void volume of **3'** estimated by *PLATON* is 40.1%. The local structure of the tetrahedral Zn<sub>4</sub>O cluster and the NTB<sup>3−</sup> unit of **3'** is similar to that of **3**, but many of the key dihedral angles in **3'** are significantly altered compared with those in **3** upon loss of guest molecules. The major difference is that the dihedral angle



**Fig. 5.** (a) The X-ray crystal structures of **3** and **3'**, which show doubly interpenetrated PdF<sub>2</sub> nets. (b) Comparison of the structures between **3** (red) and **3'** (blue). The statistically disordered structure of **3** is separated into two parts (A) and (B), and each of them is superimposed with the structure of **3'** that is not disordered. The site occupancy factors in **3** were given to 0.5 for all carboxylic oxygen atoms, 0.5 for the Zn atom that sits on a general position, and 0.1667 for the Zn atom that sits on a three-fold crystallographic axis. Thermal ellipsoids are drawn with 30% probability. (c) Rearrangements of the framework components upon guest removal and rebinding. Thermal ellipsoids are drawn with 50% probability. Colour scheme: Zn yellow, O red, N blue, C gray.

Scheme 5. Self-assembly of **4**.

**Fig. 6.** The X-ray crystal structure of  $\{[\text{Ni}(\text{cyclam})]_2[\text{BPTC}] \cdot 2\text{H}_2\text{O}\}_n$  **4**. (a) An ORTEP drawing of **4** with atomic numbering scheme. The thermal ellipsoids are drawn with 30% probability. (b) Top view seen on the (110) plane, showing the two-dimensional square grid network. (c) Side view (in CPK) showing the stacking of the two-dimensional layers. Colour scheme: Ni yellow, O (BPTC) red, N blue, C (cyclam) white, C (BPTC) green, guest water pink.

between two phenyl rings locating at the *trans* position around the  $\text{Zn}_4\text{O}(\text{CO}_2)_6$  cluster in **3'** is  $84.7(3)^\circ$ , while that in **3** is  $0^\circ$  (Fig. 5). This means that the  $\text{Zn}_4\text{O}$  cluster and  $\text{NTB}^{3-}$  units undergo significant positional and rotational rearrangements upon guest solvent removal. The crystal dynamic is triggered by the edge-to-face  $\pi$ - $\pi$  interactions between the phenyl rings that belong to two interpenetrated nets in **3'** (shortest  $\text{C} \cdots \text{C}$  distance  $3.630(9) \text{ \AA}$ , dihedral angle  $68.3(3)^\circ$ ). In **3**, there is no interaction between the two interpenetrated nets. This crystal dynamic is reversible: When the desolvated crystal is exposed to the vapor of DEF/EtOH (3/1, v/v) for 12 h, a framework structure (**3''**) the same as **3** is restored with retention of the single crystallinity.

The host framework exhibits photoluminescence whose  $\lambda_{\text{max}}$  depends on the presence or absence of the guest molecules. MOFs **3** and **3'** exhibit intense photoluminescence at  $\lambda_{\text{max}}$  433 and 463 nm, respectively, upon photo-excitation at 340 nm. The 30 nm difference in the luminescence spectra between **3** and **3'** may be attributed to the absence and presence of  $\pi$ - $\pi$  interactions, respectively, between the interpenetrated nets. In addition, the luminescence also depends on the guest identity. When desolvated solid **3'** is immersed in different solvents, the  $\lambda_{\text{max}}$  of the luminescence band appears at a different wavelength, e.g., 435 nm in pyridine, 456 nm in methanol, and 466 nm in benzene. The guest-dependent luminescence, which shows no relationship with

the binding constant of the host with the guest, cannot be clearly understood yet.

### Irreversible SC-SC Transformation Involving Various Types of Motions of Molecular Components on Removal of Guest Molecules

Although the SC-SC transformations discussed previously are mostly reversible, there are several irreversible SC-SC transformations that occur in the MOFs that have flexible and dynamic structures.<sup>[21,43]</sup>

A square-grid network,  $\{[\text{Ni}(\text{cyclam})]_2[\text{BPTC}] \cdot 2\text{H}_2\text{O}\}_n$  **4**, has been assembled from a  $[\text{Ni}^{\text{II}}(\text{cyclam})]$  complex and  $\text{BPTC}^{4-}$  ( $\text{BPTC}^{4-} = 1,1'$ -biphenyl-2,2',6,6'-tetracarboxylate, Scheme 5).<sup>[21]</sup> Solid **4** is soluble in hot water but insoluble in common organic solvents. The host is thermally stable up to  $330^\circ\text{C}$ .

The X-ray crystal structure of **4** is shown in Fig. 6. The two phenyl rings of a  $\text{BPTC}^{4-}$  unit are twisted almost perpendicularly with respect to each other (dihedral angle  $77.9(2)^\circ$ ), and each  $\text{BPTC}^{4-}$  acts as the planar four-connecting organic building block to coordinate four  $\text{Ni}^{\text{II}}$  macrocyclic complexes that act as linear linkers. The size of the square compartment in the square grid network is  $10 \text{ \AA} \times 11 \text{ \AA}$ , but the effective void size is around  $1 \text{ \AA} \times 1 \text{ \AA}$ . Therefore, the water guest molecules are intercalated between the layers instead of inside



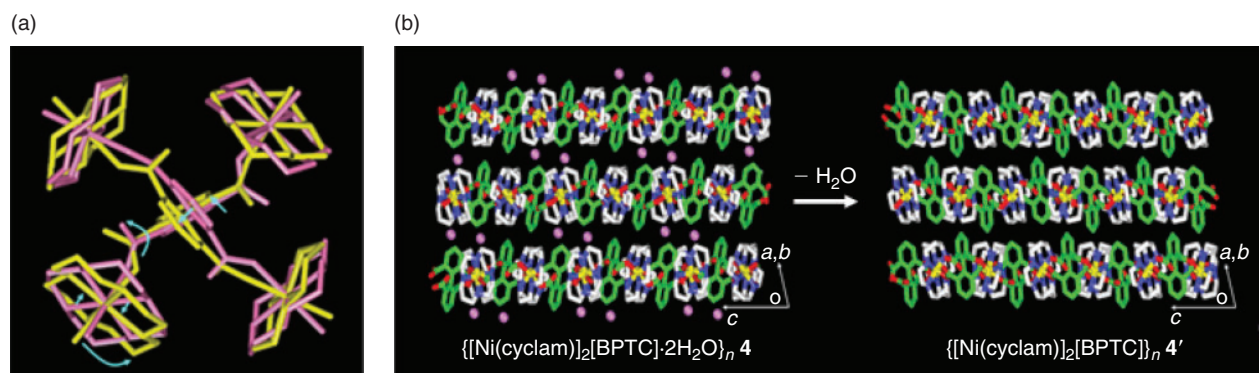


**Fig. 7.** (a) Comparison of the fundamental units of the X-ray crystal structures of **4** (pink) and **4'** (yellow) with all corresponding Ni<sup>II</sup> positions in **4** and **4'** superimposed. (b) Comparison of the stacking modes of layers in **4** and **4'**.

the square compartments. The void volume is about 12% of the total crystal volume, as estimated by using *PLATON*.

When crystal **4** is heated at 180°C under 10<sup>−5</sup> torr for 24 h, the guest water molecules intercalated between the layers are completely removed to result in desolvated solid {[Ni(cyclam)]<sub>2</sub>[BPTC]}<sub>n</sub> **4'**, with retention of the single crystallinity. The N<sub>2</sub> gas sorption data measured for **4'** indicate that it is non-porous. The X-ray powder diffraction patterns indicate that the peak that corresponds to the (110) plane appears at 2θ 9.7° for **4** is shifted to 2θ 10.2° in **4'**, which corresponds to a reduction of the interlayer distance on dehydration by 0.42 Å, from 9.03 to 8.61 Å, according to the Bragg equation. The X-ray crystal structure of **4'** is similar to that of **4**. However, significant rearrangements of the molecular components occur on removal of the water guest molecules. The fundamental units of the X-ray crystal structures of **4** and **4'** are compared in Fig. 7a by superimposing all the corresponding Ni atoms at the same positions, since all Ni atom positions in **4** are retained in **4'**. On removal of the water guest molecules intercalated between the layers, the carboxylate planes rotate along the C<sub>(phenyl)</sub>–C<sub>(carboxylate)</sub> axis. The macrocyclic rings also rotate relative to the original positions. In addition, Ni–N4 macrocyclic planes exhibit a bending motion relative to the Ni–O bond axes with retention of the Ni coordinates. The biphenyl group of BPTC<sup>4−</sup> performs a swing motion, and thus the axis that links the central carbon atoms of the BPTC<sup>4−</sup> units is shifted by 18.3° relative to the (110) plane (Fig. 7b). It is apparent that the reduction of the interlayer distance on desolvation involves various types of motions (rotation, swinging, and bending) of the molecular components in the crystal.

When crystal **4'** is immersed in water or exposed to water vapor for four days, the (110) peak of the original structure starts to be restored, although its intensity is remarkably weaker than that of the peak of the dehydrated structure. It seems that diffusion of water molecules into the dehydrated non-porous structure of **4'** is extremely slow.

## Conclusions

Retention of the single crystallinity even after the extensive rearrangement or dynamic movement of molecular

components of the crystal is quite contrary to our intuitive view, but recent studies have revealed that this occurs in some MOF crystals as a result of their flexible and dynamic structures. When a macrocyclic complex and aromatic carboxylate are employed in the assembly of MOFs, the network creates grooves between the macrocyclic complexes. The one-dimensional chains or two-dimensional layers thus assembled construct robust frameworks since the macrocycles and grooves fit together in a key and lock style. In these cases, the single crystallinity can be retained even after the removal and rebinding of the guest molecules, even if the framework shrinks or swells. In particular, when three-dimensional channels are created in the open frameworks, the single crystallinity can be easily retained even when the guest molecules are exchanged or when the framework is oxidized with the inclusion of new anions in the channels. In addition, the doubly interpenetrated PdF<sub>2</sub> net structure that is constructed by the Zn<sub>4</sub>O clusters acting as secondary building units retains its single crystallinity during many cycles of desolvation and resolution processes, even though the processes involve extensive rotational motions of the molecular components. This reversible SC-SC transformation must be attributed to the existence of the three-dimensional channels as well as to the interactions between the doubly interpenetrated nets. A two-dimensional network, which contains pores that are so small that guest molecules are intercalated between the layers, reduces the interlayer distances on desolvation. The two-dimensional network exhibits an irreversible SC-SC transformation on desolvation, which involves various types of motions (rotation, swinging, and bending) of the molecular components.

Despite these findings, we still cannot clearly explain the absorption and luminescence spectroscopic changes that depend on the presence and absence of the guest molecules as well as guest identity with the conventional coordination chemistry. In this respect, we should develop so-called nanospace chemistry that can explain how the guest molecules that are confined in nanochannels or nanopores affect the properties of the host. For this, we should collect more data and develop the theory, which will be the subjects of future work.

## Acknowledgments

This work was supported by the Korea Research Foundation Grant funded by the Korean Government (MOEHRD, Basic Research Promotion Fund, KRF-2005-084-C00020) and by the SRC program of MOST/KOSEF through the Center for Intelligent Nano-Bio Materials (Grant no. R11-2005-008-00000-0).

## References

- [1] H. K. Chae, D. Y. Siberio-Perez, J. H. Kim, Y. B. Go, M. Eddaoudi, A. J. Matzger, M. O'Keeffe, O. M. Yaghi, *Nature* **2004**, *427*, 523. doi:10.1038/NATURE02311
- [2] M. Eddaoudi, D. B. Moler, H. Li, B. Chen, T. M. Reineke, M. O'Keeffe, O. M. Yaghi, *Acc. Chem. Res.* **2001**, *34*, 319. doi:10.1021/AR000034B
- [3] M. Eddaoudi, H. Li, O. M. Yaghi, *J. Am. Chem. Soc.* **2000**, *122*, 1391. doi:10.1021/JA9933386
- [4] R. Kitaura, K. Fujimoto, S. Noro, M. Kondo, S. Kitagawa, *Angew. Chem. Int. Ed.* **2002**, *41*, 133. doi:10.1002/1521-3773(20020104)41:1<133::AID-ANIE133>3.0.CO;2-R
- [5] K. Uemura, S. Kitagawa, M. Kondo, K. Fukui, R. Kitaura, H.-C. Chang, T. Mizutani, *Chem. Eur. J.* **2002**, *8*, 3586. doi:10.1002/1521-3765(20020816)8:16<3586::AID-CHEM3586>3.0.CO;2-K
- [6] E. Y. Lee, M. P. Suh, *Angew. Chem. Int. Ed.* **2004**, *43*, 2798. doi:10.1002/ANIE.200353494
- [7] J. W. Ko, K. S. Min, M. P. Suh, *Inorg. Chem.* **2002**, *41*, 2151. doi:10.1021/IC011281U
- [8] K. S. Min, M. P. Suh, *Chem. Eur. J.* **2001**, *7*, 303. doi:10.1002/1521-3765(20010105)7:1<303::AID-CHEM303>3.0.CO;2-H
- [9] H. J. Choi, T. S. Lee, M. P. Suh, *Angew. Chem. Int. Ed.* **1999**, *38*, 1405. doi:10.1002/(SICI)1521-3773(19990517)38:10<1405::AID-ANIE1405>3.0.CO;2-H
- [10] H. J. Choi, T. S. Lee, M. P. Suh, *J. Incl. Phenom. Macrocycl. Chem.* **2001**, *41*, 155. doi:10.1023/A:1014436406651
- [11] N. L. Rosi, L. Eckert, M. Eddaoudi, D. T. Vodak, J. Kim, M. O'Keeffe, O. M. Yaghi, *Science* **2003**, *300*, 1127. doi:10.1126/SCIENCE.1083440
- [12] E. Y. Lee, S. Y. Jang, M. P. Suh, *J. Am. Chem. Soc.* **2005**, *127*, 6374. doi:10.1021/JA043756X
- [13] M. Eddaoudi, J. Kim, N. Rosi, D. Vodak, M. O'Keeffe, O. M. Yaghi, *Science* **2002**, *295*, 469. doi:10.1126/SCIENCE.1067208
- [14] K. S. Min, M. P. Suh, *J. Am. Chem. Soc.* **2000**, *122*, 6834. doi:10.1021/JA000642M
- [15] O. M. Yaghi, H. Li, *J. Am. Chem. Soc.* **1996**, *118*, 295. doi:10.1021/JA953438L
- [16] L. Pan, H. Liu, X. Lei, X. Huang, D. H. Olson, H. J. Turro, J. Li, *Angew. Chem. Int. Ed.* **2003**, *42*, 542. doi:10.1002/ANIE.200390156
- [17] T. Sawaki, Y. Aoyama, *J. Am. Chem. Soc.* **1999**, *121*, 4793. doi:10.1021/JA9900407
- [18] M. Albrecht, M. Lutz, A. L. Spek, G. van Koten, *Nature* **2000**, *406*, 970. doi:10.1038/35023107
- [19] J. A. Real, E. Andrés, M. C. Munoz, M. Julve, T. Granier, A. Bousseksou, F. Varret, *Science* **1995**, *268*, 265.
- [20] H. R. Moon, J. H. Kim, M. P. Suh, *Angew. Chem. Int. Ed.* **2005**, *44*, 1261. doi:10.1002/ANIE.200461408
- [21] M. P. Suh, H. R. Moon, E. Y. Lee, S. Y. Jang, *J. Am. Chem. Soc.* **2006**, *128*, 4710. doi:10.1021/JA056963L
- [22] K. Biradha, M. Fujita, *Angew. Chem. Int. Ed.* **2000**, *39*, 3843. doi:10.1002/1521-3773(20001103)39:21<3843::AID-ANIE3843>3.0.CO;2-#
- [23] B. F. Abrahams, P. A. Jackson, R. Robson, *Angew. Chem. Int. Ed.* **1998**, *37*, 2656. doi:10.1002/(SICI)1521-3773(19981016)37:19<2656::AID-ANIE2656>3.0.CO;2-M
- [24] B. Rather, M. J. Zaworotko, *Chem. Commun.* **2003**, 830. doi:10.1039/B301219K
- [25] B. Chen, M. Eddaoudi, T. M. Reineke, J. W. Kampf, M. O'Keeffe, O. M. Yaghi, *J. Am. Chem. Soc.* **2000**, *122*, 11559. doi:10.1021/JA003159K
- [26] O. Ohmori, M. Kawano, M. Fujita, *J. Am. Chem. Soc.* **2004**, *126*, 16292. doi:10.1021/JA046478A
- [27] S. S.-Y. Chui, S. M.-F. Lo, J. P. H. Charmant, A. G. Orpen, I. D. Williams, *Science* **1999**, *283*, 1148. doi:10.1126/SCIENCE.283.5405.1148
- [28] B. F. Abrahams, M. Moylan, S. D. Orchard, R. Robson, *Angew. Chem. Int. Ed.* **2003**, *42*, 1848. doi:10.1002/ANIE.200250633
- [29] S. Kitagawa, R. Kitaura, S. Nori, *Angew. Chem. Int. Ed.* **2004**, *43*, 2334. doi:10.1002/ANIE.200300610
- [30] M. P. Suh, J. W. Ko, H. J. Choi, *J. Am. Chem. Soc.* **2002**, *124*, 10976. doi:10.1021/JA017560Y
- [31] H. J. Choi, M. P. Suh, *J. Am. Chem. Soc.* **2004**, *126*, 15844. doi:10.1021/JA0466715
- [32] K. Biradha, M. Fujita, *Angew. Chem. Int. Ed.* **2002**, *41*, 3392. doi:10.1002/1521-3773(20020916)41:18<3392::AID-ANIE3392>3.0.CO;2-V
- [33] C. J. Kepert, M. J. Rosseinsky, *Chem. Commun.* **1999**, 375. doi:10.1039/A809746A
- [34] K. Biradha, Y. Hongo, M. Fujita, *Angew. Chem. Int. Ed.* **2002**, *41*, 3395. doi:10.1002/1521-3773(20020916)41:18<3395::AID-ANIE3395>3.0.CO;2-D
- [35] K. Takaoka, M. Kawano, M. Tominaga, M. Fujita, *Angew. Chem. Int. Ed.* **2005**, *44*, 2151. doi:10.1002/ANIE.200462214
- [36] C.-D. Wu, W. Lin, *Angew. Chem. Int. Ed.* **2005**, *44*, 1958. doi:10.1002/ANIE.200462711
- [37] B. F. Abrahams, M. J. Hardie, B. F. Hoskins, R. Robson, G. A. Williams, *J. Am. Chem. Soc.* **1992**, *114*, 10641. doi:10.1021/JA00052A073
- [38] J.-P. Zhang, Y.-Y. Lin, W.-X. Zhang, X.-M. Chen, *J. Am. Chem. Soc.* **2005**, *127*, 14162. doi:10.1021/JA054913A
- [39] S. Lidin, M. Jacob, S. Anderson, *J. Solid State Chem.* **1995**, *114*, 36. doi:10.1006/JSSC.1995.1005
- [40] M. P. Suh, *Adv. Inorg. Chem.* **1997**, *44*, 93.
- [41] R. Robson, *J. Chem. Soc., Dalton Trans.* **2000**, 3735. doi:10.1039/B003591M
- [42] M. O'Keeffe, M. Eddaoudi, H. Li, T. M. Reineke, O. M. Yaghi, *J. Solid State Chem.* **2000**, *152*, 3. doi:10.1006/JSSC.2000.8723
- [43] E. J. Cussen, J. B. Claridge, M. J. Rosseinsky, C. J. Kepert, *J. Am. Chem. Soc.* **2002**, *124*, 9574. doi:10.1021/JA0262737